



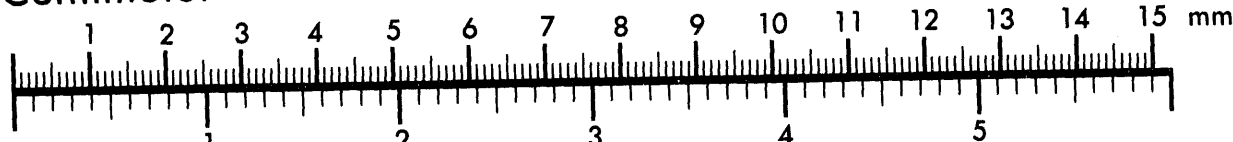
## AIM

Association for Information and Image Management

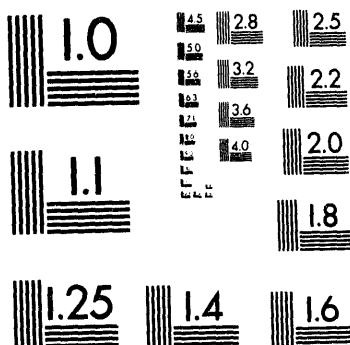
1100 Wayne Avenue, Suite 1100  
Silver Spring, Maryland 20910

301/587-8202

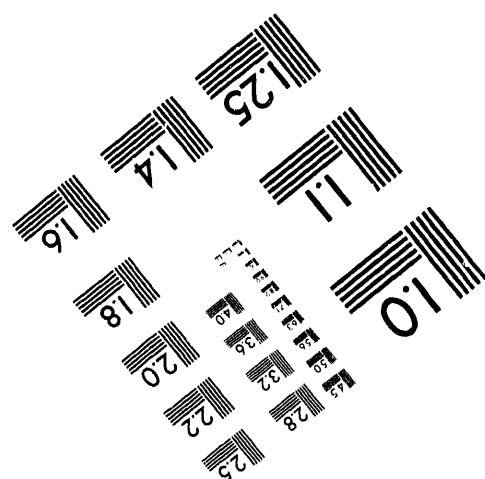
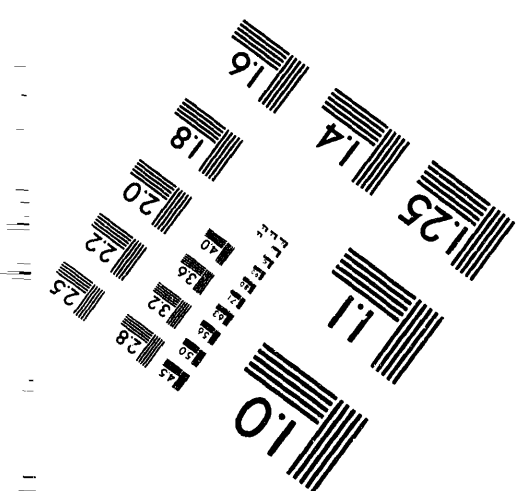
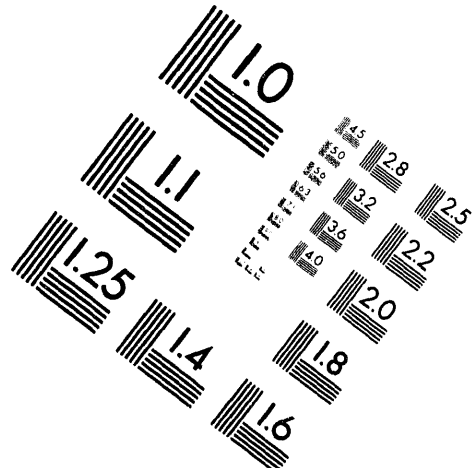
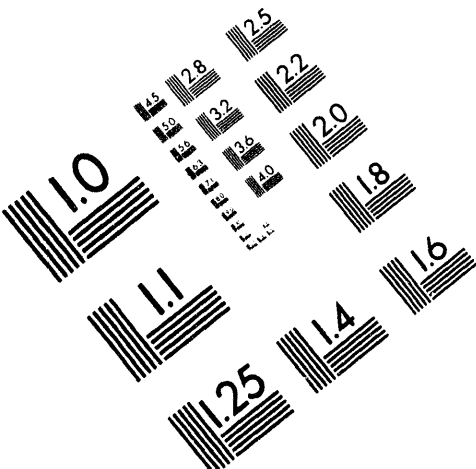
## Centimeter



## Inches



MANUFACTURED TO AIIM STANDARDS  
BY APPLIED IMAGE, INC.



1 of 1

Conf-940142-45

**Superconducting Superlattices and Multilayers  
Part of SPIE's  
OE\*LASE '94  
Los Angeles, California  
January 22-28, 1994**

"The submitted manuscript has been authored by a contractor of the U.S. Government under contract No. DE-AC05-84OR21400. Accordingly, the U.S. Government retains a nonexclusive, royalty-free license to publish or reproduce the published form of this contribution, or allow others to do so, for U.S. Government purposes."

## **ENERGY GAP STRUCTURE OF LAYERED SUPERCONDUCTORS**

**S. H. Liu and R. A. Klemm**

**SOLID STATE DIVISION  
OAK RIDGE NATIONAL LABORATORY  
Managed by  
MARTIN MARIETTA ENERGY SYSTEMS, INC.  
Under  
Contract No. DE-AC05-84OR21400  
With the  
U. S. DEPARTMENT OF ENERGY  
OAK RIDGE, TENNESSEE**

**December 1993**

### **DISCLAIMER**

This report was prepared as an account of work sponsored by an agency of the United States Government. Neither the United States Government nor any agency thereof, nor any of their employees, makes any warranty, express or implied, or assumes any legal liability or responsibility for the accuracy, completeness, or usefulness of any information, apparatus, product, or process disclosed, or represents that its use would not infringe privately owned rights. Reference herein to any specific commercial product, process, or service by trade name, trademark, manufacturer, or otherwise does not necessarily constitute or imply its endorsement, recommendation, or favoring by the United States Government or any agency thereof. The views and opinions of authors expressed herein do not necessarily state or reflect those of the United States Government or any agency thereof.

Se

**DISTRIBUTION OF THIS DOCUMENT IS UNLIMITED**

# Energy gap structure of layered superconductors

S. H. Liu

Solid State Division, Oak Ridge National Laboratory  
Oak Ridge, TN 37831-6032

and

R. A. Klemm

Materials Science Division, Argonne National Laboratory  
Argonne, IL 60439

## ABSTRACT

We report the energy gap structure and density-of-states (DOS) of a model layered superconductor with one superconducting layer and one normal layer in a unit cell along the  $c$ -axis. In the physically interesting parameter range where the interlayer hopping strengths of the quasiparticles are comparable to the critical temperature, the peaks in the DOS curve do not correspond to the order parameter (OP) of the superconducting layer, but depend on the OP and the band dispersion in the  $c$ -direction in a complex manner. In contrast to a BCS superconductor, the DOS of layered systems have logarithmic singularities. Our simulated tunneling characteristics bear close resemblance to experimental results.

## 1. INTRODUCTION

A common feature shared by all copper oxide based high- $T_c$  superconductors is their highly stratified crystal structure. This influences the electronic structure in such a way that the quasiparticles move freely within the layers but hop weakly between layers. Many authors have analyzed the connection between the layered structure and the superconducting properties of the materials, which are more complex than low- $T_c$  superconductors.<sup>1-11</sup> For instance, the theories predict that in the weak hopping limit in which the interlayer hopping strengths of the quasiparticles are weak compared with the critical temperature  $T_c$ , the density-of-states (DOS) curves have peaks at the energy gaps or order parameters (OP's) of the individual layers.<sup>1-2</sup> In the strong hopping limit, however, the main features in the DOS curve should be identified with the OP's of the bands.<sup>3-5</sup> The present authors have studied the interesting and perhaps most relevant parameter range where the hopping strengths are comparable to the OP's or  $T_c$  for a two-layer model for which both layers are superconducting but with different pair coupling strengths.<sup>10-11</sup> It was found that the results of both weak hopping and strong hopping theories are incomplete and potentially misleading. The features in the DOS are not directly identifiable with the OP's of the layers, but are shifted and modified by the band dispersion along the  $c$ -direction. The singularities in the DOS curves are logarithmic, which are less pronounced than those for BCS superconductors. We conclude that the tunneling curves for layered superconductors should be interpreted with caution. In this paper we report a similar analysis of a two-layer S-N model in which one layer is superconducting and one layer is normal. There is only one OP for the superconducting layer, yet the DOS curve shows the same kind of complex structure as reported by us previously. It gives further support to our contention that the structure of the DOS as observed in tunneling experiments is sensitive to the  $c$ -axis band structure. Furthermore, the DOS curve has the V-shaped bottom around zero bias and nonvanishing zero bias conductance, as observed in many experiments.

## 2. THEORY

The model consists of two conducting layers, one superconducting (S) and one normal (N), in a unit cell with identical two-dimensional band structures. Two different interlayer hopping strengths  $J_1$  and  $J_2$  are assumed. The

quasiparticles within the S layer interact via a phenomenological pairing interaction of the BCS type so that the total Hamiltonian has the form  $H = H_0 + V$ , where the band energy term is

$$H_0 = \sum_{j \mathbf{k} \sigma} \sum_{n=1}^2 \xi_0(\mathbf{k}) \psi_{jn\sigma}^\dagger(\mathbf{k}) \psi_{jn\sigma}(\mathbf{k}) + \sum_{j \mathbf{k} \sigma} [J_1 \psi_{j1\sigma}^\dagger(\mathbf{k}) \psi_{j2\sigma}(\mathbf{k}) + J_2 \psi_{j2\sigma}^\dagger(\mathbf{k}) \psi_{j+1,1\sigma}(\mathbf{k}) + H.c.], \quad (1)$$

where  $\xi_0(\mathbf{k}) = \mathbf{k}^2/2m_0 - E_F$ ,  $\mathbf{k} = (k_x, k_y)$ ,  $\sigma$  is the spin index,  $n = 1, 2$  is the layer index within a unit cell, and the sum on  $j$  is over all unit cells normal to the planes. The units are chosen such that  $\hbar = k_B = 1$ . The interaction term is

$$V = -\frac{1}{2} \sum_j \sum_{\mathbf{k}\sigma} \sum_{\mathbf{k}'\sigma'} \lambda_0 \psi_{j1\sigma}^\dagger(\mathbf{k}) \psi_{j1\sigma'}^\dagger(-\mathbf{k}) \psi_{j1\sigma'}(-\mathbf{k}') \psi_{j1\sigma}(\mathbf{k}'), \quad (2)$$

where the S layer is labelled by 1 and the pair coupling strengths  $\lambda_0$  is cut off at an energy  $\omega_{||}$ . The condition  $\sigma' = -\sigma$  will be imposed, since the pair coupling mechanism only allows singlet pairs. The model, sketched schematically in Fig.1, is a generalized version of the S-N model proposed by Abrikosov except that two different hopping strengths are introduced.<sup>7</sup> One can go one step further by invoking different two-dimensional band structures and different Fermi surfaces for the two layers,<sup>8</sup> but the simpler model considered here is sufficient for bringing out the physical picture.

The quasiparticle Green's function matrix elements are defined in the familiar way:

$$G_{nn'}(\mathbf{k}, \tau - \tau') = -\langle T[\psi_{n\sigma}(\mathbf{k}, \tau) \psi_{n'\sigma}^\dagger(\mathbf{k}, \tau')]\rangle, \\ F_{nn'}(\mathbf{k}, \tau - \tau') = \langle T[\psi_{n\sigma}(\mathbf{k}, \tau) \psi_{n',-\sigma}(-\mathbf{k}, \tau')]\rangle, \quad (3)$$

where  $\mathbf{k} = (\mathbf{k}, k_z)$ ,  $k_z$  is the crystal momentum in the  $c$ -direction,  $\langle \dots \rangle$  denotes thermal average, and

$$\psi_{n\sigma}(\mathbf{k}) = \Omega^{1/2} \sum_{k_z} \psi_{jn\sigma}(\mathbf{k}) e^{ik_z[js + (n-1)d]}. \quad (4)$$

In the above equation  $\Omega$  is the volume of the crystal,  $s$  is the thickness of the unit cell in the  $c$ -direction, and  $d$  is the separation between layer 1 and layer 2 within the same cell. The separation between adjacent layers in adjacent cells will be denoted by  $d' = s - d$ . The spin index is suppressed in the Green's function matrix elements. We define the order parameter  $\Delta$  for the S layered by

$$\Delta = \lambda_0 \sum_{k'} \langle \psi_{1\sigma}(\mathbf{k}') \psi_{1,-\sigma}(-\mathbf{k}') \rangle. \quad (5)$$

The inverse of the Green's function matrix has the form

$$\hat{G}^{-1}(\mathbf{k}, \nu) = \begin{pmatrix} i\nu - \xi_0(\mathbf{k}) & -g(k_z) & \Delta & 0 \\ -g^*(k_z) & i\nu - \xi_0(\mathbf{k}) & 0 & 0 \\ \Delta^* & 0 & i\nu + \xi_0(\mathbf{k}) & g(k_z) \\ 0 & 0 & g^*(k_z) & i\nu + \xi_0(\mathbf{k}) \end{pmatrix}, \quad (6)$$

where the quantity

$$g(k_z) = J_1 e^{ik_z d} + J_2 e^{-ik_z d'} \equiv \epsilon_\perp(k_z) e^{-i\phi(k_z)}, \quad (7)$$

with

$$\epsilon_\perp(k_z) = [J_1^2 + J_2^2 + 2J_1 J_2 \cos k_z s]^{1/2}, \quad (8)$$

$$\phi(k_z) = \frac{J_2 \sin k_z d' - J_1 \sin k_z d}{J_2 \cos k_z d' + J_1 \cos k_z d}. \quad (9)$$

The functions  $\pm \epsilon_\perp(k_z)$  represent the dispersion of the two tight-binding bands in the  $c$ -direction.

The inversion of the Green's function matrix is straightforward. Putting the results in Eq.(3), we deduce the following gap equation:

$$\Delta = \frac{\lambda_0}{\beta} \sum_{\mathbf{k}\nu} \frac{[\nu^2 + \xi_0^2(\mathbf{k})]\Delta}{D}, \quad (10)$$

where  $\beta = 1/T$ ,  $T$  is the temperature, and the sum on  $\nu$  is over the Matsubara frequencies under the constraint that  $|\nu| < \omega_{||}$ . The quantity  $D$  is the determinant of the inverse Green's function matrix:

$$D = (\nu^2 + \xi_0^2)^2 + 2\epsilon_1^2(\nu^2 - \xi_0^2) + \epsilon_1^4 + |\Delta|^2(\nu^2 + \xi_0^2). \quad (11)$$

We will choose the OP to be real. The subsequent integration over the two-dimensional bands brings in the density-of-states factor  $N(0) = m_0/2\pi s$ , but  $\epsilon_{\perp}(\mathbf{k}_s)$  remains explicitly in the gap equation. Consequently, the  $c$ -axis dispersion of the quasi-particle bands enters the superconducting properties.

The critical temperature  $T_c$  is solved from the linearized version of Eq.(11). In the limit of zero hopping the critical temperature is solved from

$$\lambda_0 N(0) a_{||}(T_{c0}) = 1, \quad (12)$$

where  $a_{||}(T) = \ln(2\gamma\omega_{||}/\pi T)$ , and  $\gamma = 1.78$ . We use  $T_{c0}$  to set the energy scale in our numerical analysis. With increasing hopping  $T_c$  is lowered steadily from the zero hopping limit  $T_{c0}$ . In the limit of strong hopping, i.e.  $J_1, J_2 \gg \omega_{||}$ , the critical temperature is solved from

$$\frac{1}{2} \lambda_0 N(0) a_{||}(T_c) = 1. \quad (13)$$

It can be seen that  $T_c < T_{c0}$ . For intermediate hopping strengths the dependence of  $T_c$  on  $J$ 's for a fixed  $J_1/J_2 = 0.5$  is shown in Fig.2

The OP at zero temperature depends also on the hopping strengths. In the zero hopping limit, Eq.(11) reduces to the BCS gap equation for the S layer alone. With increasing hopping  $\Delta$  decreases steadily as shown in Fig.3. The curve is calculated for the same set of parameters as in Fig.2.

In Fig.4 we show  $\Delta(T)$  for the same of model parameters except for fixed  $J_2/T_{c0} = 1$ . For these parameters the critical temperature  $T_c = 0.854T_{c0}$ . The quantity  $\Delta(T)$  has the typical BCS temperature dependence.

The density-of-states in the superconducting state is calculated in the standard way:

$$N_s(\omega) = \frac{1}{\pi} \sum_{\mathbf{k}\nu} \text{Im}G_{11}(\mathbf{k}, \nu)|_{\nu \rightarrow -i\omega + \delta}, \quad (14)$$

where  $\delta = 0^+$ . The detail of this calculation has been reported elsewhere,<sup>11</sup> so we will merely discuss the results here. In Fig.5 we show a set of total DOS curves at zero temperature for the same model parameters in Fig.1 with  $J_2/T_{c0}$  ranging from a weak hopping value of 0.1 to a strong hopping value of 5. The calculated OP's are marked on the graph with arrows. The four curves are displaced vertically by 2 units successively. In the weak hopping case, the bottommost curve, the DOS consists of a BCS-type superconducting part superimposed on a uniform background of one unit, which is the DOS of the normal layer. Thus, the S and N layers are essentially independent of one another. The next higher curve corresponds to a higher hopping, and it shows that a small and ill-defined gap structure develops in the N layer by the proximity effect, although the OP is only in the S layer. The third curve from the bottom clearly shows two sets of peaks, with the inner peaks sharper and more prominent than the outer peaks. Furthermore, neither sets of peaks coincides with the OP. In the top curve the outer peaks are hardly noticeable, and the inner peaks are at approximately  $\pm\Delta/2$ . We have identified previously that the two sets of peaks are derived from two types of pairing when the local, single-layer electron wavefunctions are projected onto the band states for the entire crystal.<sup>10,11</sup> The inner peaks mark the energy of the intraband pairs for which both quasiparticles are in the same band, while the outer peaks measure the energy of the interband pairs where the two quasiparticles are in opposite bands. The latter contains the band dispersion in the  $c$ -direction, therefore the peaks are broader

and exhibit fine structure. All except the top curve are gapless in the sense that the conductance at zero bias is nonvanishing. The two middle ones have the V-shaped bottom as seen in many tunneling experiments.<sup>12-15</sup> We conclude that the DOS of multilayer superconductors is intrinsically complex as a result of the band structure in the *c*-direction, and it is inappropriate to interpret the structure as evidence of multiple gaps.

We have discussed in previous publications that the DOS vanishes inside the threshold values  $\pm\omega_0''$ , where<sup>10-11</sup>

$$\omega_0'' = \frac{\Delta}{2} \sqrt{1 - \frac{\Delta^2}{4(J_2 - J_1)^2}}. \quad (15)$$

The system is gapless if  $\Delta > 2|J_1 - J_2|$ , because  $\omega_0''$  is imaginary. The inner peaks appear at  $\pm\omega_0'$  where

$$\omega_0' = \frac{\Delta}{2} \sqrt{1 - \frac{\Delta^2}{4(J_2 + J_1)^2}}. \quad (16)$$

The peaks are logarithmic singularities, i.e.

$$N_s(\omega) = A_{\pm} \ln |\omega - \omega_0'| + B_{\pm}, \quad (17)$$

where  $A_{\pm}, B_{\pm}$  are nonsingular in  $\omega$  and  $\pm$  refer to the outside or inside of the singularities. A second set of logarithmic singularities occur at  $\pm\omega_+'$ , where

$$\omega_+'' = \frac{1}{2} [\sqrt{4(J_1 + J_2)^2 + \Delta^2} + \Delta]. \quad (18)$$

Both singularities are less sharp than the power-law  $(\omega^2 - \Delta^2)^{-1/2}$  singularity of a BCS superconductor.

The tunneling characteristics at various temperatures are calculated by convoluting the DOS curve with the Fermi distribution factor:

$$\frac{dI(V)}{dV} \propto \int N_s(\omega - eV) \frac{\beta e^{\beta\omega}}{(e^{\beta\omega} + 1)^2} d\omega, \quad (19)$$

where  $e$  is quasiparticle charge and  $V$  is the bias. We show in Fig.6 a set of tunneling characteristics for the same set of material parameters used in Fig.4. The temperatures are marked on the curves. At elevated temperatures the fine details of the DOS curves tend to be smoothed away, with only a shallow dip left around zero bias. These curves resemble qualitatively the *ab*-axes tunneling data of BSCCO<sup>12,13</sup>. The temperature sensitive features inside of the main peaks seen in YBCO remain unexplained,<sup>14,15</sup> but they may indicate interlayer pairing.<sup>3,4,11</sup>

### 3. SUMMARY AND CONCLUSIONS

We have demonstrated that, simply as a result of the layered structure, the copper-oxide superconductors may have multiple peaks in their density of states and tunneling characteristics. As a result, tunneling data should be analyzed with caution. Because the short *c*-axis coherence lengths, one is more likely to observe the bulk behavior by tunneling out of the *a* and *b*-planes.

Our theoretical results, though limited in scope, can shed light on real materials. Many high- $T_c$  materials have more than one  $\text{CuO}_2$  layers in a unit cell with other intervening layers which may become superconducting. Consider a material with  $m$  identical superconducting layers and  $n$  normal layers. In the zero hopping limit the critical temperature  $T_{c0}$  is determined by  $\lambda_0$  of the *S* layers according to Eq.(12). In the strong hopping limit, however, the effective coupling constant is  $m\lambda_0/(m+n)$ , which is the average over all *S* and *N* layers.<sup>3-5</sup> Therefore, within the same family of materials, we expect higher  $T_c$  in a material with more *S* layers.

More layers in a unit cell also result in more bands in the *c*-direction. Without solving the more than two layer model in detail, we anticipate that the main DOS peaks are due to intraband pairing and should be logarithmic singularities. On the other hand, there should be more interband pairing features, each associated with a different

pair of bands, resulting in a set of less distinct outer peaks. Only the dip outside the main peak remains as a remnant of the multilayer nature of the material. It is interesting to note that the layered organic superconductor  $\kappa$ -(BEDT-TTF)<sub>2</sub>Cu(NCS)<sub>2</sub> displays the same double peak tunneling characteristic although its critical temperature is merely 11K.<sup>16</sup> We view this as added evidence that the crystal geometry, rather than the coupling mechanism, is the cause of the observed complex gap structure.

#### 4. ACKNOWLEDGMENTS

This work was supported by the U.S. Department of Energy, Division of Basic Energy Sciences, under contracts no. DE-AC005-84OR21400 with Martin Marietta Energy Systems, Inc., and no. W-31-109-ENG-38.

#### REFERENCES

1. M. Tachiki, S. Takahashi, F. Steglich and H. Adrian, *Z. Phys. B*, Vol. **80**, pp. 161-166, 1990.
2. L. N. Bulaevskii and M. V. Zyskin, *Phys. Rev. B*, Vol. **42**, pp. 10230-10234, 1990.
3. R. A. Klemm and S. H. Liu, *Physica C*, Vol. **176**, pp. 189-194, 1991.
4. R. A. Klemm and S. H. Liu, *Phys. Rev. B*, Vol. **44**, pp. 7526-7545, 1991.
5. S. H. Liu and R. A. Klemm, *Phys. Rev. B*, Vol. **45**, pp. 415-430, 1992.
6. R. A. Klemm and S. H. Liu, *Physica C*, Vol. **191**, pp. 383-398, 1992.
7. A. A. Abrikosov, *Physica C*, Vol. **182**, pp. 191-202, 1991.
8. A. A. Abrikosov and R. A. Klemm, *Physica C*, Vol. **191**, pp. 224-236, 1992.
9. S. H. Liu and R. A. Klemm, *Phys. Rev. B*, Vol. **48**, pp. 4080-4094, 1993.
10. S. H. Liu and R. A. Klemm, *Phys. Rev. B*, Vol. **48**, pp. 10650-10652, 1993.
11. S. H. Liu and R. A. Klemm, *Physica C*, Vol. **216**, pp. 293-304, 1993.
12. H. J. Tao, A. Chang, F. Lu, and E. L. Wolf, *Phys. Rev. B*, Vol. **45**, pp. 10622-10632, (1992).
13. Q. Chen and K.-W. Ng, *Phys. Rev. B*, Vol. **45**, pp. 2569-2572, 1992.
14. M. Gurvitch, J. M. Valles, Jr., A. M. Cuolfo, R. C. Dynes, J. P. Gorno, L. F. Schneemeyer and J. V. Waszczak, *Phys. Rev. Lett.*, Vol. **63**, pp. 1008-1011, 1989.
15. J. M. Valles, Jr., R. C. Dynes, A. M. Cuolfo, M. Gurvitch, L. F. Schneemeyer, J. P. Gorno, and J. V. Waszczak, *Phys. Rev. B*, Vol. **44**, pp. 11986-11996, 1991.
16. H. Bando, S. Kashiwaya, H. Tokumoto, H. Anzai, N. Kinoshita and K. Kajimura, *J. Vac. Sci. Technol.*, Vol. **A 8**, pp. 479-483, 1990.

## FIGURE CAPTIONS

Fig. 1. Schematic diagram of the two-layer S-N model.

Fig. 2. The dependence of the critical temperature  $T_c$  on the hopping strengths for the S-N model. The model parameters are displayed in the graph.

Fig. 3. The dependence of the order parameter  $\Delta$  on the hopping strengths for the S-N model. The model parameters are displayed in the graph.

Fig. 4. The temperature dependence of the order parameter  $\Delta(T)$  for the S-N model with  $J_2/T_{c0} = 1$ .

Fig. 5. A set of density-of-states (DOS) curves at zero temperature for the S-N model. The model parameters are given in Fig. 2. The curves are displaced vertically by 2 units successively.

Fig. 6. Simulated tunneling characteristics for the S-N model whose model parameters are in Fig. 2. The curves are displaced vertically by 2 units successively.

ORNL-DWG 93-15790R

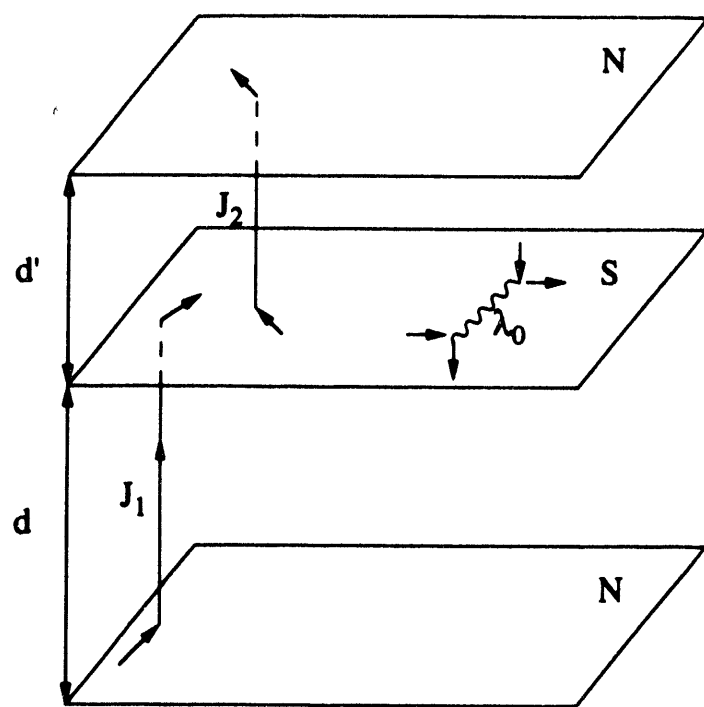


Fig. 1

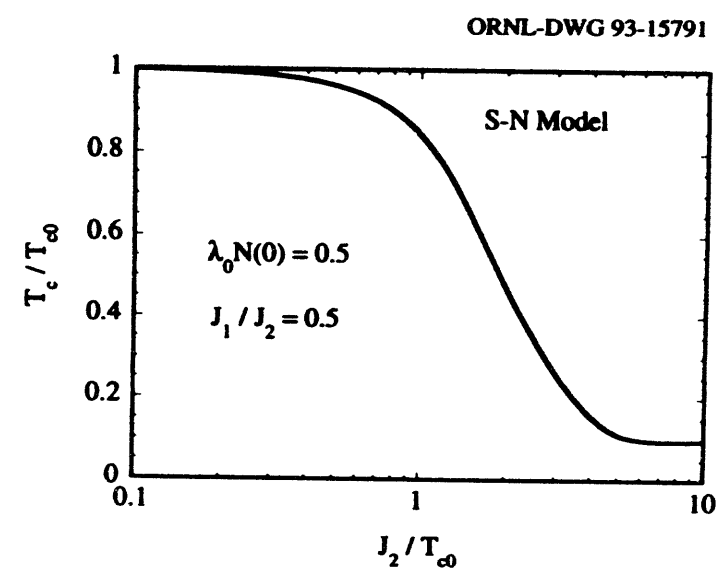


Fig. 2

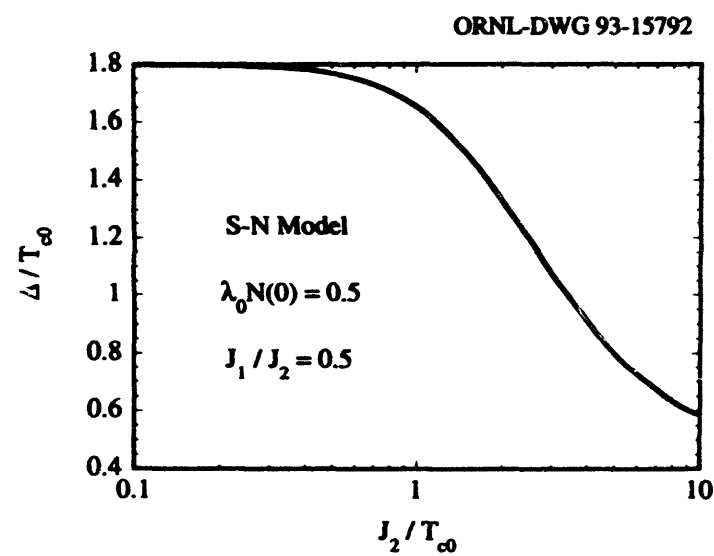


Fig. 3

ORNL-DWG 93-15794

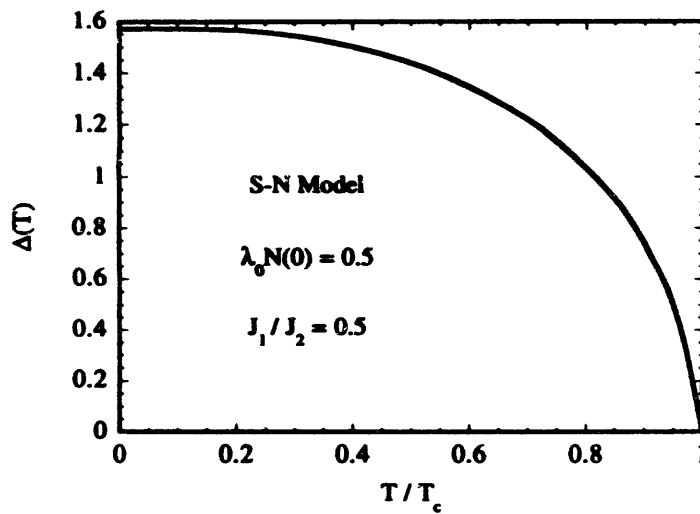


Fig. 4

ORNL-DWG 93-15793R

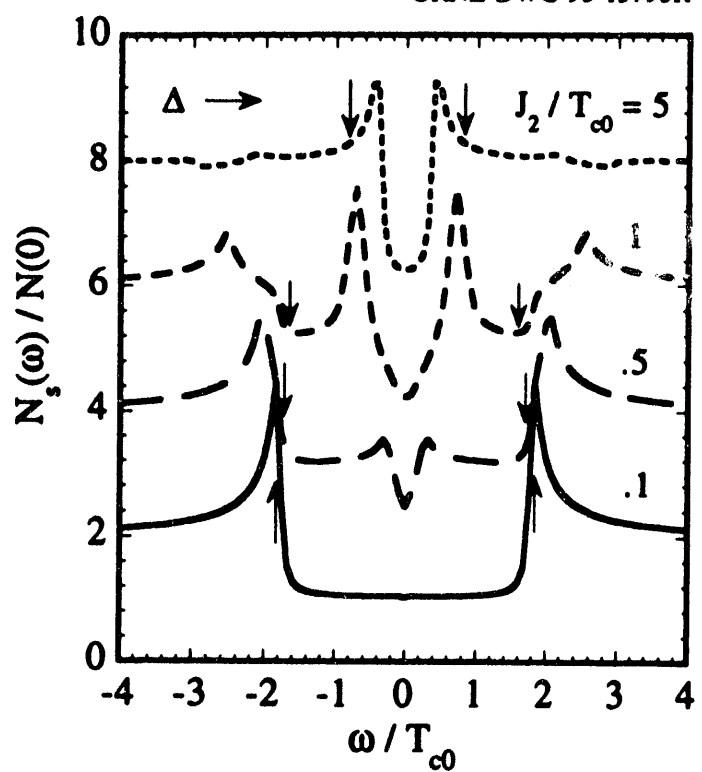


Fig. 5

ORNL-DWG 93-15795

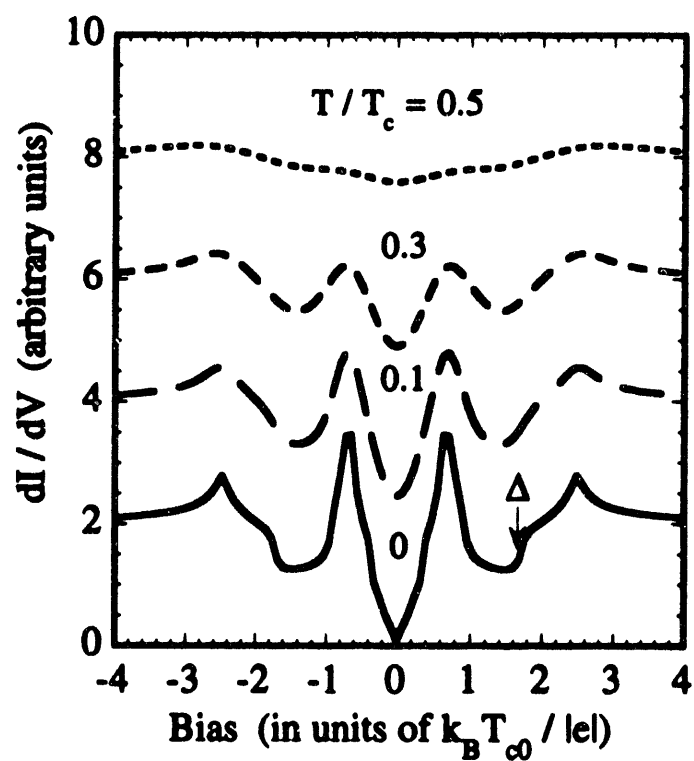


Fig. 6

100  
1000  
10000  
100000  
1000000

DATE  
ENDING  
10/14/94

